

Paleomagnetism of the Western Saharan Basins: An Overview



M. E. M. Derder, B. Henry, S. Maouche, N. E. Merabet, M. Amenna and B. Bayou

Abstract Numerous paleomagnetic studies were performed in the western Saharan basins, particularly during the last decades. Primary magnetization of the sedimentary formations older than Bashkirian appeared as totally overprinted. By contrast, 23 new coherent paleomagnetic poles, mainly from Bashkirian to Autunian age and from Middle Triassic to Lias age, were determined. These new data greatly improved the Apparent Polar Wander Path (APWP) for Africa, and consequently for the whole Gondwana, especially for the Upper Carboniferous. The corresponding paleoreconstruction strongly argued for an A2 Pangea during this last period. By its comparison with paleomagnetic data from undated geological units, this new APWP provided dating of these units. Paleomagnetic data highlighted also the existence of a post-Liassic regional tectonic event having affected the Paleozoic cover in the Sahara platform. Finally, several magnetic overprints, pointed out in these studies, are of chemical origin, with likely a significant role of ground-fluids. Indeed, fluids migration phenomena often favored chemical changes and remagnetization process. Upper Carboniferous, Permian and Upper Cretaceous–Cenozoic overprinting ages were thus probably linked to regional geochemical events that occurred in the Saharan Platform.

Keywords Paleomagnetism · Sahara · Basins · Geodynamic · Tectonics
Geochemistry

M. E. M. Derder (✉) · S. Maouche · N. E. Merabet · M. Amenna · B. Bayou
CRAAG, B.P. 63, 16340 Bouzaréah, Algiers, Algeria
e-mail: m.e.m.derder@gmail.com

B. Henry

Paléomagnétisme, Institut de Physique du Globe de Paris, Sorbonne Paris Cité,
Univ. Paris Diderot and UMR 7154 CNRS, 4 avenue de Neptune,
94107 Saint-Maur cedex, France

© Springer Nature Switzerland AG 2019

A. Bendaoud et al. (eds.), *The Geology of the Arab World—An Overview*,
Springer Geology, https://doi.org/10.1007/978-3-319-96794-3_7

291

1 Introduction

The geodynamical evolution of the Hoggar shield since the Precambrian is highly linked to that of the surrounding Saharan basins. It has conditioned the formation and the evolution of these basins during the Phanerozoic (Fabre 2005 and references herein). The paleomagnetism can be considered as one of the best tools for studying such evolution. Since post-Hercynian tectonic events in the Saharan Platform are still considered as a matter of debate (e.g., Haddoum et al. 2001), it could point out such movements, which should be related to reactivation of the deep mega-shear zones of the Hoggar (Bertrand and Caby 1978; Black et al. 1994; Liégeois et al. 1994). Then, it could specify the Phanerozoic evolution of the Hoggar basement.

On one hand, it is well known that the paleomagnetism is also a powerful tool to determine drift of the main tectonic plates and to provide paleocontinental reconstructions (e.g., Van der Voo 1993; McElhinny et al. 2003; Derder et al. 2006; Torsvik et al. 2012; Henry et al. 2017). Thus, it could give a global vision of the Paleozoic drift patterns of whole Gondwana and of the African plate after the opening of the Atlantic Ocean. The migration of these continents could also have an impact on the Hoggar tectonic evolution (e.g., Liégeois et al. 2005).

At the end of the 1980's, very few paleomagnetic data were available from the Hoggar surroundings (Morel et al. 1981; Daly and Irving 1983; Kent et al. 1984; Aifa et al. 1990), and the Apparent Polar Wander Path (APWP) of the African plate was poorly defined, especially for the Paleozoic times. The Gondwana APWP was also doubtful for this period, leading to the existence of very different APWPs for this supercontinent (e.g., Smith and Hallam 1970; Van der Voo and French 1974; Morel and Irving 1981; Smith et al. 1981; Bachtadse and Briden 1991; Schmidt and Clark 2000). From a geodynamical point of view, the convergence model of Gondwana and Laurussia plates during the Upper Paleozoic interval remained hypothetical. The evolution pattern of the Pangea supercontinent from Carboniferous to Triassic was still controverted (e.g., Torcq et al. 1997).

To improve, by a better constraint of APWP, the knowledge of the geodynamical evolution of the Pangea, Gondwana, and Africa plates, numerous paleomagnetic studies were performed in the stable Saharan Platform during the last decades. Many areas were thus investigated, i.e., Tindouf, Bechar–Abadla, Mezarif, Timimoun, Reggane, Ahnet-Mouydir, Illizi, Murzuq, Tin Serririne, and Taoudeni basins surrounding the Hoggar shield (see Fig. 1; Tables 1 and 2). In this chapter, we present an overview of the paleomagnetic studies conducted in these basins of the Saharan Platform and highlight their different geodynamical, structural, geochemical, and chronological implications.

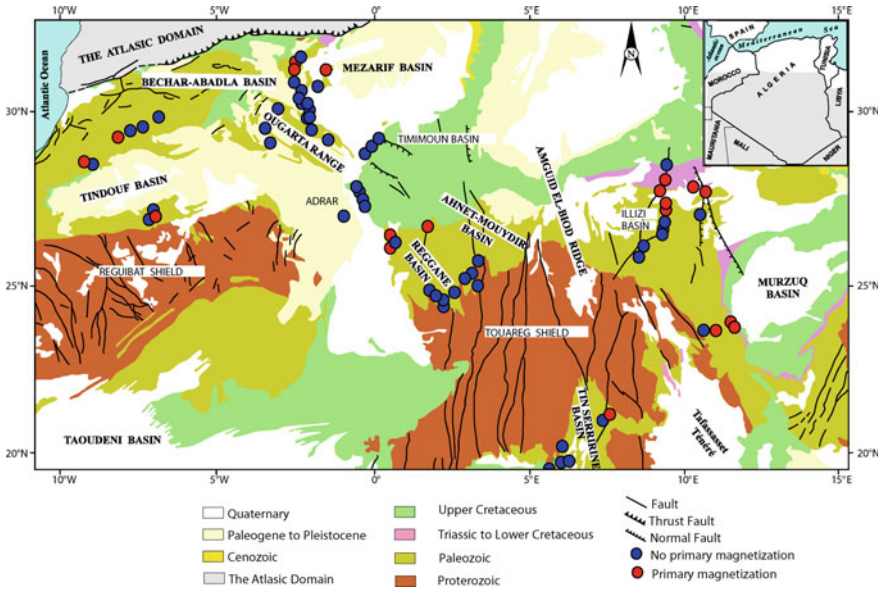


Fig. 1 Geological map of the studied Saharan basins; paleomagnetic sites yielding primary magnetization are in red (full) dots, whereas those giving remagnetizations or unstable remanences are in blue (open) dots. Locations for two studies (Kent et al. 1984; Boudzoumou et al. 2011), evidencing remagnetizations, far on the western and southern borders of the Taoudeni basin are out of the limits of the map

2 Geological Setting

The Saharan Platform is a Precambrian basement unconformably overlain by transgressive Phanerozoic thick deposits. Various tectonic events delineated sedimentary basins having their own more or less complete stratigraphic sedimentary column (Fabre 2005; Haddoum et al. 2001). The stratigraphic correlations between the basins highlight lateral facies changes and discontinuities. These basins contain mainly Paleozoic deposits, Mesozoic and Cenozoic sediments being scarce (Conrad and Le Mosquet 1984). The Paleozoic sediments reach thicknesses of over 8000 m in the Tindouf Basin, 6000 m in Reggane one and up to 8000 m in the Bechar Basin. From lithological point of view, the Cambrian formations consist of sandstones, quartzites, and conglomerates, deposited over the infra-Cambrian crystalline basement. The overlying formations up to the Upper Carboniferous are represented by various facies (shales, sandstones, limestones, etc), mainly marine and with some sedimentary gaps. The Stephano–Autunian formations essentially consist of red beds. There is a large pre-Mesozoic sedimentation gap. The Triassic is represented by sandy shales and lacustrine–continental deposits unconformably overlying the Paleozoic formations. When present, the Jurassic formations are present in the form of marine and lacustrine to continental deposits. The transgressive

Table 1 Paleomagnetic data from Saharan Platform associated with primary magnetization

Basin	Rock unit	Site	Age	<i>N</i>	Reliability	Paleomagnetic pole	References
Tindouf	Djebel Reoutiana	28.9°N, 8.0°W	Namurian	NS		28.4°S, 56.9°E, <i>K</i> = 642, <i>A</i> ₉₅ = 1.7°	Merabet et al. (1999)
	Merkala	28.5°N, 8.5°W	Low. Stephanian Autunian	9		32.4°S, 56.6°E, <i>K</i> = 399 <i>A</i> ₉₅ = 2.3°	Henry et al. (1999)
	Dolerites dykes	27.1°N, 7.0°W	198.9 ± 1.8 Ma (Chabou 2008)	10 17		69.8°S, 62.1°E, <i>K</i> = 490, <i>A</i> ₉₅ = 2.0°	Boussada et al. (2015)
	Ben Zireg	31.2°N, 1.8°W Ben Zireg	Fannian	3 3	Fold test	19.2°N, 19.8°E, <i>A</i> ₉₅ = 3.7°	Aifa et al. (1990)
Bechar- Abadla	Low unit of Abadla	31°N, 2.7°W	Autunian	11 12		29.1°S, 57.8°E, <i>K</i> = 462, <i>A</i> ₉₅ = 2.0°	Merabet et al. (1998)
	Up. unit of Abadla	31°N, 2.7°W	Autunian	13 13		29.0°S, 60.0°E, <i>A</i> ₉₅ = 5°	Morel et al. (1981)
	Up. unit of Abadla	31°N, 2.7°W	Autunian	1 1	Coherence with Morel et al. (1981)	29.2°S, 60.0°E,	Merabet et al. (1998)
	Nekheila	31.4°N, 1.5°W	Autunian	7 7	Fold test with Abadla	29.3°S, 56.4°E, <i>K</i> = 322, <i>A</i> ₉₅ = 3.40	Merabet et al. (2000, 2005)
Reggane	Ain Ech Chebbi	26.5°N, 0.3°W Ain Chebbi	Low. Moscovian	4 4		22.9°S, 51.8°E, <i>K</i> = 123, <i>A</i> ₉₅ = 6.6°	Daly and Irving (1983)
	Ain Ech Chebbi	26.5°N, 0.3°W Ain Chebbi	Low. Serpukhovian-Low. Moscovian	10 18	Fold test + reversal test	26.5°S, 44.7°E, <i>K</i> = 383, <i>A</i> ₉₅ = 4.7°	Derder et al. (2001a)
	Dolerites	26.5°N, 0.3°W Ain Chebbi	195.0 ± 1.6 Ma (Chabou et al. 2007)	20 24	Fold test "synfolding"	57.6°N, 254.3°E,	Smith et al. (2006)

(continued)

Table 1 (continued)

Basin	Rock unit	Site	Age	N	Reliability	Paleomagnetic pole	References
Ahmet	Hassi Bachir	26.6°N, 1.0°E Hassi Bachir	Up. Namurian–Low. Moscovian	NS		26.8°S, 56.6°E, K = 204, A ₉₅ = 3.7°	Daly and Irving (1983)
				7	7		
Illizi	Hassi Bachir	26.6°N, 1.8°E Hassi Bachir	Up. Namurian–Low. Moscovian	15	Fold test	32.8°S, 55.7°E, K = 328, A ₉₅ = 2.0°	Derder et al. (2009)
				28			
	Up. Oubarakat Low. El Adeb Larache	27.5°N, 8.8°E; El Adeb Larache	Bashkirian	7		28.2°S, 55.5°E, K = 207, A ₉₅ = 3.4°	Derder et al. (2001b)
				24			
El Adeb Larache	27.45°N, 8.9°E El Adeb Larache	Moscovian	10		28.7°S, 55.8°E, K = 235, A ₉₅ = 2.9°	Henry et al. (1992)	
			18				
El Adeb Larache	27.4°N, 9.5°E Edjeleh	Moscovian	6	Fold test	28.3°S, 58.9°E, K = 157, A ₉₅ = 4.2°	Derder et al. (2001c)	
Low. Tiguentourine	7.7°N, 9.0°E La Reculée	Stephano–Autunian	10		35.3°S, 60.3°E, K = 195, A ₉₅ = 3.2°	Derder et al. (1994)	
			19				
Low. Zarzaitine	27.9°N, 9.3°E La Reculée	Carnian–Rhaetian	8	Reversal test	70.9°S, 55.2°E, K = 478, A ₉₅ = 2.3°	Kies et al. (1995)	
Mid. Zarzaitine	28°N, 9.7°E Zarzaitine	Liassic	14		71.8°S, 54.9°E, K = 91, A ₉₅ = 3.9°	Derder et al. (2001d)	
			21				

(continued)

Table 1 (continued)

Basin	Rock unit	Site	Age	<i>N</i>	Reliability	Paleomagnetic pole	References
Murzuq	Up. Dombaba	23.5°N, 11.9°E In Ezzane	Lower Moscovian	NS 12 12	Fold test	25.2°S, 59.9°E, <i>K</i> = 55, <i>A</i> ₉₅ = 5.4°	Amenna et al. (2014)
	Zarzaïtine	24.2°N, 11.5°E Anai	<i>Up. Permian</i>	11 14	*	43.8°S, 70.9°E, <i>K</i> = 80, <i>A</i> ₉₅ = 4.5°	Henry et al. (2014)
Tin Serririne	Gabbro sill	24°0N, 10°4E Arrikine	<i>Low. Devonian</i>	10 13	Contact test	42.8°S, 22.9°E, <i>K</i> = 88, <i>A</i> ₉₅ = 4.7°	Derder et al. (2016)
	dolerites sills and dykes	21.1°N, 7.38°E 20.8°N, 6.46°E	347.6 ± 16.2 Ma (Djellit et al. 2006)	12 33		18.8°S, 31.2°E, <i>K</i> = 29, <i>A</i> ₉₅ = 7.5°	Derder et al. (2006)

Italics in "Age" column correspond to age from paleomagnetic dating. *N* (number of sites yielding primary magnetization), NS (number of studied sites), Symbol "°" indicates reliable variation of the paleomagnetic direction, related to stratigraphical level

Table 2 Paleomagnetic data from Saharan platform (a) associated with “published” remagnetizations data, (symbol “?” means that age remains doubtful or undetermined, possibly related to composite magnetizations), or (b) with “unpublished” remagnetizations or unstable magnetization data (Merabet Nacer Eddine, Pers. com. for all basins except Tin Serririne; and Derder Mohamed El Messaoud, Pers. com for Tin Serririne Basin)

Basin	Rock unit	Coordinates	Age of main remagnetizations	References
(a)				
Tindouf	Djebel Reouiana	28.9°N, 8.0°W	Permian	Merabet et al. (1999)
	Merkala	28.5°N, 8.5°W	Permian	Henry et al. (1999)
	Dolerites dykes	27.1°N, 7.0°W	Cenozoic	Boussada et al. (2015)
Bechar– Abadla	Famenian	31.9°N, 0.8°E	Tournaisian + Permian	Aifa et al. (1990); Aifa (1993)
	Lower Devonian	29.7°N, 2.1°W		
Ougarta	Magmatic complexes	29.8°N, 2.7°E	Tournaisian + Viséan	Lamali et al. (2013)
		30.2°N, 3.2°W		
		29.2°N, 1.2°W		
Timimoun	Up. Viséan	29.3°N, 02° E	Cenozoic	Kherroubi (2003)
Ahnet	Givetian Hazzel Matti	24.9°N, 2.2°E	Cenozoic + ?	Smith et al. (1994)
	Famennian– Tournaisian	26.8°N, 0.4°E		
	Frasnian	26.7°N, 0.7°E	Cenozoic	Bayou et al. (2000)
			Liassic Dogger?	
			Carboniferous + ?	
	Givetian	26.7°N, 1.0°E	Cenozoic	Carboniferous? + ?
			Carboniferous? + ?	
Emsian	26.7°N, 0.9°E	Cenozoic	Carboniferous? + ?	
		Liassic Dogger?		
		Carboniferous? + ?		
Hassi Bachir	26.7°N, 1.8°E	Permian	Daly and Irving (1983)	
		Mesozoic	Derder et al. (2009)	

(continued)

Table 2 (continued)

Basin	Rock unit	Coordinates	Age of main remagnetizations	References
Illizi	Albian sandstone and clay	28.7°N, 9.2°E	Cenozoic	Henry et al. (2004b)
	Liassic limestone and clay	27.9°N, 9.3°E		
	Up. Triassic-Rhaetian sandstone	27.8°N, 9.3°E		
	Stephano–Autunian clays	27.8°N, 9.0°E		
	Moscovian limestone and clay	27.6°N, 9.8°E		
	Bashkirian limestone and clay	27.3°N, 8.8°E		
	Namurian limestone	27.2°N, 8.7°E		
	Visean sandstone	27.0°N, 8.7°E		
	Tournaisian sandstone	26.8°N, 8.8°E		
	Tournaisian red beds	26.7°N, 8.9°E		
	Strunian sandstone	26.6°N, 9.0°E		
	Strunian shelled limestone	26.4°E, 8.5°E		
	Givetian limestone	26.3°N, 8.5°E		
	Emsian sandstone	26.4°N, 8.4°E		
	Silurian sandstone	26.2°N, 9.1°E		
Low. Devonian	26.3°N, 8.2°E	Lamali et al. (2014)		
Silurian	25.7°N, 7.9°E			
Murzuq	Low. Silurian	24.0°N, 10.5°S	Cenozoic	Amenna et al. (2017)
	Up. Ordovician			

(continued)

Table 2 (continued)

Basin	Rock unit	Coordinates	Age of main remagnetizations	References
Tin Serririne	Givetian	20.0°N, 6.0°E	Cenozoic	Amenna (2009)
			Jurassic?	Bayou et al. (2004).
			Carboniferous?	
	Emsian		Cenozoic	Amenna (2009)
	Low. Devonian	20.0°N, 6.0°E	Liassic?	
21.1°N, 7.4°E			Carboniferous?	Bayou et al. (2004)
Cambrian Ignimbrites	19.9°N, 6.0°E	Jurassic? + ?		
Taoudeni	Devonian Gneiguira	18.0°N, 12.3 W	?	Kent et al. (1984)
	Up. Proterozoic– Cambrian Mejeira	17.9°N, 12.3°W	?	
	Neoproterozoic	11.2°N, 4.3°W	?	Boudzoumou et al. (2011)
Basin	Rock unit	Coordinates	Age of main remagnetizations	
(b)				
Tindouf	Westphalian	28.5°N, 8.5°W	Permian	
	Up. Visean	28.6°N, 8.6°W		
	Low. Visean Strunian Silurian	29.1°N, 7.3°W	Cenozoic	
	Strunian Tournaisian Visean	26.7°N, 7.5°W	Cenozoic	
Bechar Abadla	Bashkirian Namurian Visean	31.6°N, 2.2°W	Cenozoic	Permian
	Bashkirian Moscovian	31.6°N, 2.4°W	Cenozoic	
	Moscovian	31.0°N, 2.7°W		
	Visean Namurian	30.9°N, 2.0°W		
Ougarta	Up. Visean	30.4°N, 2.3°W	Cenozoic	
	Up. Visean	30.4°N, 2.3°W	Cenozoic	
	Strunian	30.0°N, 2.1°W		
	Famenian	30.2°N, 2.2°W	Permian	
	Emsian	29.9°N, 2.1°W	Jurassic	
Timimoun	Up. Visean Tournaisian	29.4°N, 0.2°E	Cenozoic	

(continued)

Table 2 (continued)

Basin	Rock unit	Coordinates	Age of main remagnetizations
	Strunian		
Adrar	“Gothlandian” Low. Devonian Mid. Devonian	29.0°N, 0.3°W	Cenozoic Carboniferous + Permian Permian + Jurassic
	Visean Namurian	27.2°N, 0.1°W	Permian
Illizi	Cambro–Ordovician	24.5°N, 9.5°E	Cenozoic
Tin Serririne	Silurian	19.7°N, 5.8°E	Cenozoic
		20.9°N, 7.4°E	
	Ordovician	19.9°N, 5.8°E	

Upper Cretaceous shaly sandstone and carbonate sequence are found over the Saharan Platform. The Cenozoic formations are represented by clastic continental sediments from Oligocene to Pliocene and Quaternary.

The Bechar Basin is bounded to the north by the High Atlas and to the south by the Ougarta mountain range. Tindouf and Reggane basins are asymmetrically located on the N and NE of the Reguibat shield. The basement has been encountered in some deep wells in the Illizi and Ahnet area. This basement, structured as several crustal blocks by major faults under the Paleozoic sedimentary cover, would be (Freulon 1964; Beuf et al. 1971; Fabre 2005) the following:

- The Western Neoproterozoic of the Hoggar, under the Ahnet-Timimoun basins.
- The Central Hoggar, Polycyclic Paleoproterozoic, under the Amguid-El Biod Ridge.
- The Eastern Hoggar, Precambrian, under the Illizi Basin.
- The West African Craton under the Tindouf and Reggane basins.

In the Saharan Platform, basin inversion, uplift and reactivation of regional to local structures are documented as mainly related to the Hercynian collisional event (Haddoum et al. 2001). Recent observations highlight evidence of permanent mobility of this platform (Nedjari et al. 2011). Many tectonic events during different periods are linked to the basin's location, particularly for those of the western ones. During the Hercynian period, the configuration, evidenced by new structural elements, shows the platform as a foreland regarding the Variscan chain, which was edified and later eroded. The Saharan Platform is structured into synclyses. In the northwestern Sahara, the Bechar–Abadla basin is considered as atypical because of extreme mobility due to location close to the suture zone of the Variscan orogeny. This basin represents an appropriate model of foredeep basin (Nedjari et al. 2011).

It is highly subsident with very thick sedimentary filling. The deformations within the platform have been explained by distal effects of stresses generated by collision and mechanical coupling between the Gondwana and Laurussia plates. Basin exhumation and compressional reactivation of structures also occurred during the Tertiary collision between the African and European plates (Liégeois et al. 2005; Galeazzi et al. 2010).

3 Sampling and Analysis Procedure

Depending on outcropping conditions and on facies features, different stratigraphic levels of the studied geological formations were mostly sampled. To have significant and reliable data, at least seven sites were generally selected (Table 1). In favorable cases, more than 300 cores distributed on up to 33 independent sites have been drilled in the same rock unit. In most cases, the sampling was made by a portable gasoline-powered drill. Large hand samples (precisely oriented using a plaster cap) were also collected when the facies was too friable and cores were drilled in the laboratory. All samples were oriented with magnetic and sun compasses. One to three specimens of standard size (cylinders of 11 cm³) were cut from each core, allowing demagnetization treatments and additional rock magnetic studies to be performed. Prior to any demagnetization analysis, the specimens were put in a zero field for at least 1 month, in order to reduce possible viscous magnetization.

The Remanent Magnetization was mostly measured using JR4 or JR5 spinner magnetometer (AGICO, Brno, Czech Republic). In each study, whatever the kind of the rocks (sedimentary or volcanic) both thermal and Alternating Field (AF) demagnetization were performed on pilot specimens, and, when needed, by combined AF-thermal procedure. In order to correctly isolate and identify the magnetization components, numerous demagnetization steps were used (10 °C, and until 5 °C increment in high temperatures when necessary).

The results of demagnetization analysis were carried out using classical methods: they were presented on orthogonal vector plots (As and Zijderveld 1958; Zijderveld 1967). The remaining vectors after each step and the difference vectors removed between two consecutive demagnetization steps were plotted on equal area projections. When applicable, the remagnetization circles methods (Halls 1976, 1978; McFadden and McElhinny 1988), were also used. The direction of the magnetization components was calculated by principal component analysis (Kirschvink 1980). Fisher (1953) statistics were used to determine the mean characteristic directions. When appropriate, progressive unfolding was performed, allowing fold test (e.g., McElhinny 1964; McFadden 1990; Tauxe and Watson 1994). “Synfolding” magnetizations were analyzed using small circles method (Shipunov 1997; Henry et al. 2004a; Waldhör and Appel 2006). When applicable, reversal (McFadden and McElhinny 1990) and contact tests were also performed.

4 Rock magnetism

Rock magnetism analyses were carried out on all the studied geological formations. Representative samples from each formation were chosen to determine their magnetic mineralogy from different magnetic approaches, based on thermal demagnetization curves, thermomagnetic $K(T)$ curves (magnetic susceptibility as a function of temperature), and hysteresis loops. Mean susceptibility and $K(T)$ curves were determined on AGICO KLY2 (or KLY3), CSL and CS2 (or CS3) equipments and hysteresis loops on a laboratory-made translation inductometer for small samples (about 3 cm^3) within an electromagnet.

The results showed that, generally, for sedimentary formations, the main magnetic mineral carriers were hematite (Fig. 2a, b), magnetite (Fig. 3a, b) or a mixture of these two minerals (Fig. 4a, b). For the magmatic formations, rock experiments result suggested that Ti-poor titanomagnetites of pseudo-single-domain grain size (Derder et al. 2016), or a mixing of Ti-rich titanomaghemite and magnetite are the main carriers (Derder et al. 2006).

5 Paleomagnetic Results

During the demagnetization process, the analysis of the natural remanent magnetization gave different kinds of evolution on the Zijderveld plot, after elimination of a viscous component. The first one (i) is illustrated by a stable magnetic direction characteristic of a single component (Fig. 5a). The second type (ii) shows the

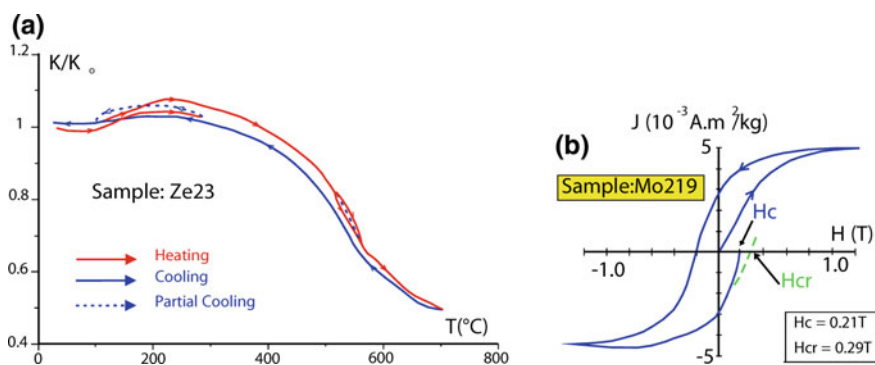


Fig. 2 **a** Typical thermomagnetic (variation of the normalized magnetic susceptibility K/K_0 during a cycle of progressive heating and cooling in air in low magnetic field) curve for ZE23 sample pointing out presence of hematite (from Fig. 3a of Derder et al. 2001d, modified). **b** Hysteresis loop for Mo219 sample (H : magnetic field; H_c : coercive force; H_{cr} : remanent coercive force; all in Tesla; J : Magnetization) suggesting presence of hematite (from Fig. 2b of Derder et al. 2001c, modified)

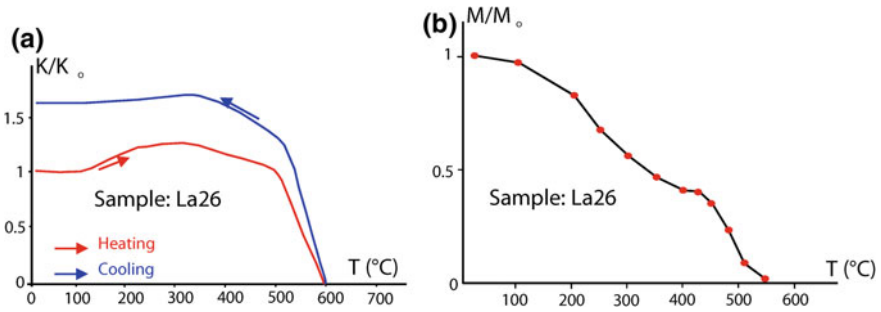


Fig. 3 **a** Thermomagnetic curve (see Fig. 2a caption) for La26 sample pointing out presence of magnetite (from Fig. 3a of Henry et al. 1992, modified). **b** Typical thermal demagnetization curve for La26 sample pointing out existence of magnetite (from Fig. 3b of Henry et al. 1992, modified)

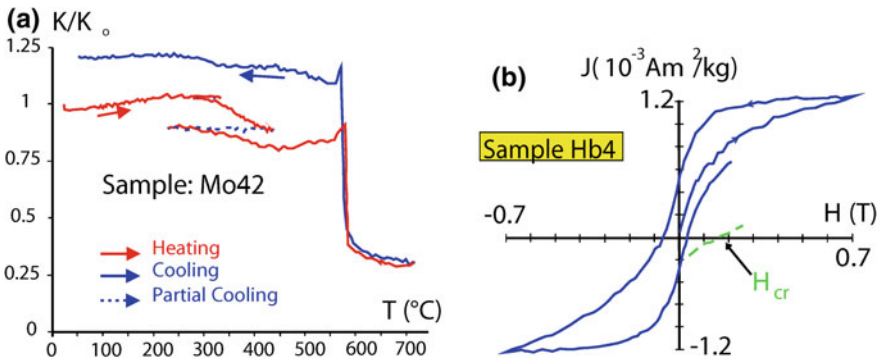


Fig. 4 **a** Typical thermomagnetic curve (see Fig. 2a caption) for Mo42 sample showing, in addition to an “Hopkinson” peak related to magnetite, the presence of hematite (from Fig. 3 of Derder et al. 2001c, modified). **b** Hysteresis loop (see Fig. 2b caption) for Hb4 sample showing wasp-waisted shape suggesting existence of magnetite and hematite (from Fig. 3b of Derder et al. 2009, modified)

isolation of several components distributed over the unblocking temperature spectra (Fig. 5b). The third one (iii) points out magnetic directions evolving along a great circle and reaching a “stable endpoint” direction for the highest demagnetization steps (Fig. 5c). The fourth one (iv) is characterized by directions evolving along a great circle (superimposition of unblocking spectra for at least two components), but no stable component was reached even for the highest demagnetization steps (Fig. 5d). Finally, the last kind (v) is characterized by an erratic behavior of the magnetization.

According to the sites, the percentage of usable data (i, ii, iii, and sometimes iv) is very variable from one study to another (e.g. Table 1). Reliability criteria (Van der Voo 1990; Henry et al. 2017) and paleomagnetic tests yielded separation of

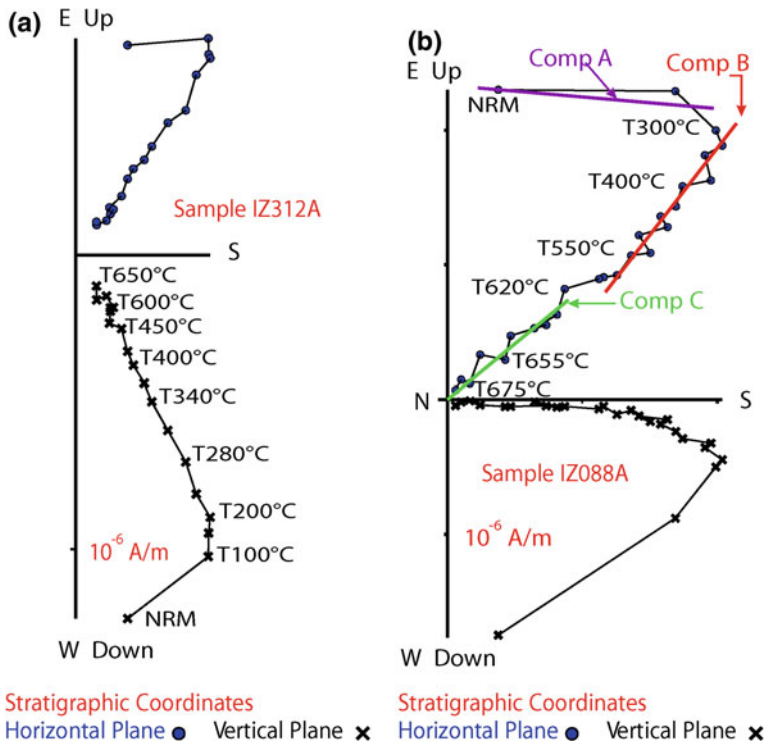


Fig. 5 Orthogonal vector plots (filled circles: horizontal plane, crosses: vertical plane), in stratigraphic coordinates for **a** samples IZ312A (from Fig. 6a of Amenna et al. 2014, modified); **b** sample: IZ088A (from Fig. 6a of Henry et al. 2014, modified); **c** sample D332 (from Fig. 6 of Derder et al. 2006, modified) and **d** sample TG019A (from Fig. 6e of Derder et al. 1994, modified)

primary (Fig. 1; Table 1) and secondary (Table 2) magnetizations. Used tests (see Table 1) were fold test (Aifa et al. 1990; Derder et al. 2001a, c, 2009; Merabet et al. 2005; Smith et al. 2006; Amenna et al. 2014) (Fig. 6), reversal test (Derder et al. 2001a) (Fig. 7) and contact test (Derder et al. 2016) (Fig. 8). Significant variability of the paleomagnetic direction pointed out in different stratigraphic levels within a same formation was also used as a criterion to highlight primary magnetization (e.g., Henry et al. 2014). Several examples (e.g., Bayou et al. 2000; Bouabdallah et al. 2003) of data of type *i* appeared to be composite (i.e., resulting from superimposition of different magnetization components with similar blocking characteristic spectra). In some favorable cases, separation of these components was possible (Merabet et al. 1999; Henry et al. 1999; Derder et al. 2001d). In all, 93 geological formations or intrusions were studied, giving 23 new paleomagnetic poles related to primary magnetizations.

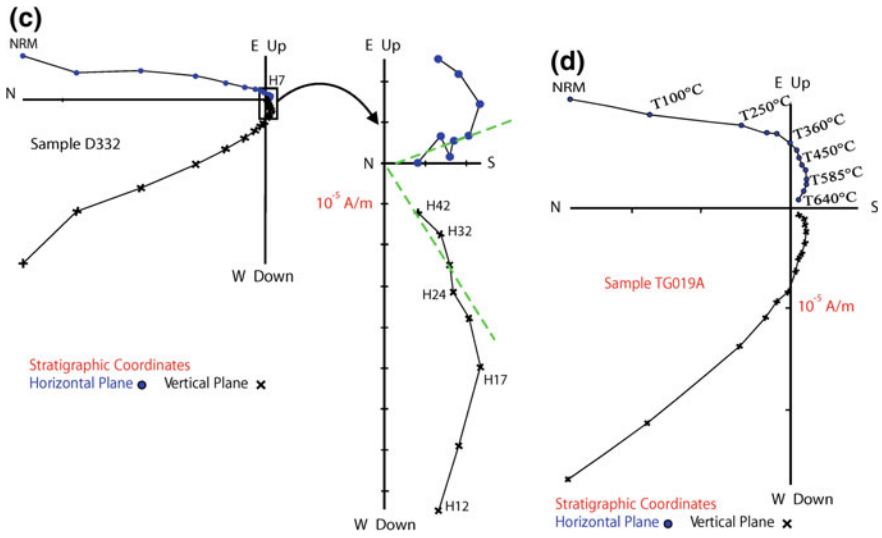


Fig. 5 (continued)

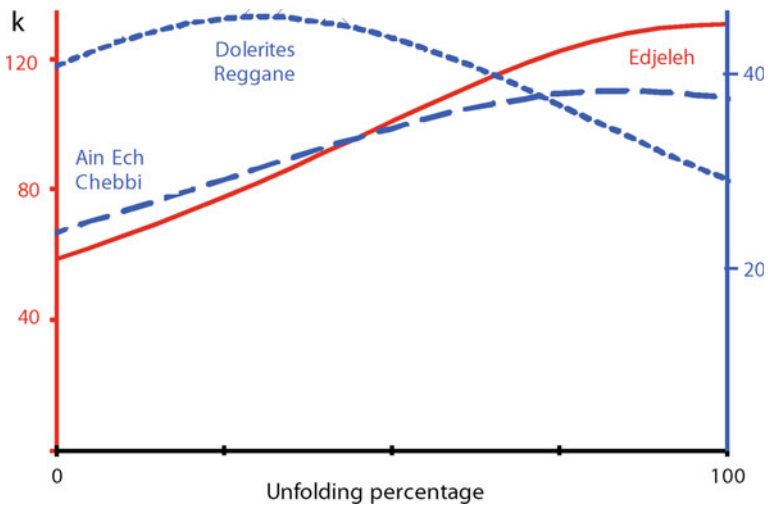


Fig. 6 Variation of k parameter (Fisher 1953) during progressive unfolding for the Moscovian Formation at Edjeleh in Illizi basin (Derder et al. 2001c), Jurassic dolerites in Reggane basin (Smith et al. 2006) and lower Serpukhovian—lower Moscovian Ain Ech Chebbi formation in Ahnet basin (Derder et al. 2009)

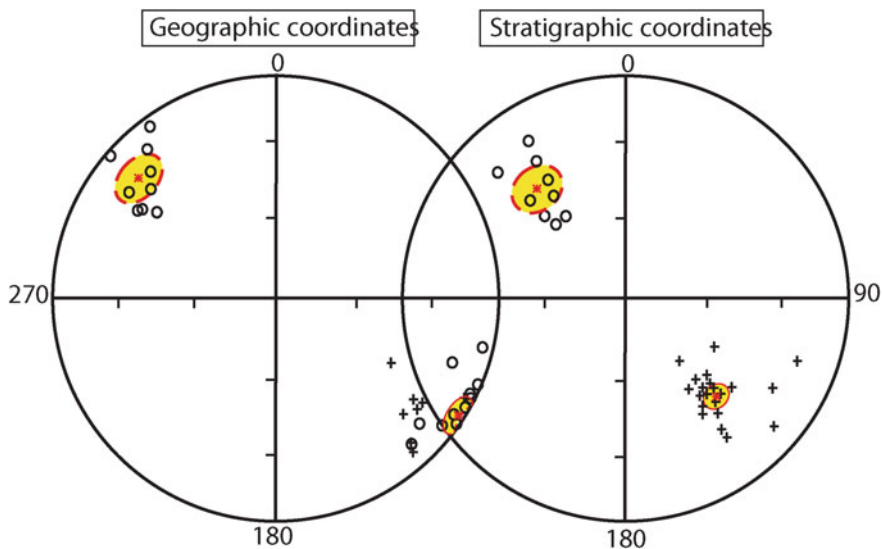


Fig. 7 Equal area plot (crosses: positive inclinations, open circles: negative inclinations) of paleomagnetic directions of middle–upper Carboniferous formations from Reggane basin. The reversal test (McFadden and McElhinny 1990) is positive after dip correction, with angular difference γ (5.0°) between mean directions for normal and reversed data lower than the critical value γ_c (9.2°), but this test is negative ($\gamma = 17.8^\circ$; $\gamma_c = 10.7^\circ$) before dip correction (from Fig. 9a of Derder et al. 2001a, modified)

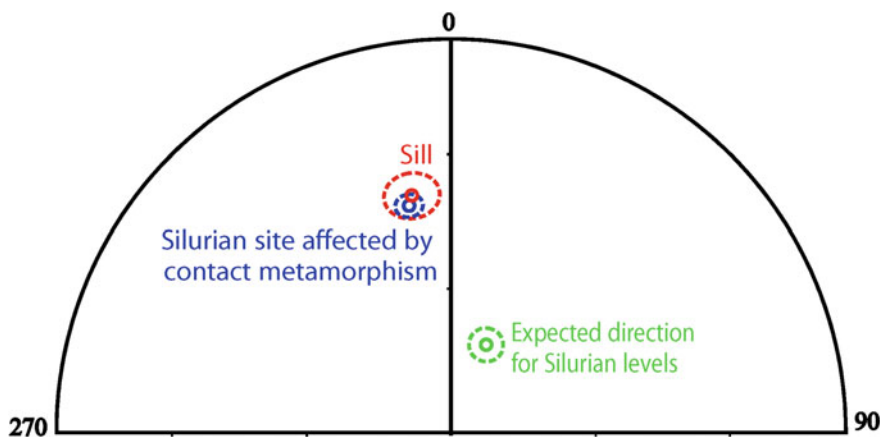


Fig. 8 Equal area plot (open circles: negative inclinations) of paleomagnetic directions obtained from the sill, after dip correction, from the sedimentary Silurian site affected by contact metamorphism and that of the expected direction of the Silurian levels (calculated from the APWP for 430 Ma), showing positive contact test

6 Discussion

6.1 *Apparent Polar Wander Path (APWP) for the Gondwana and Its Implications*

Unfortunately, all studies from dated geological units older than the Bashkirian did not yield primary magnetization, except for the Lower Carboniferous dolerites of the Tin Serririne basin (Derder et al. 2006). In addition, because of the lack of existing geological formations during several periods, the paleomagnetic poles obtained in dated formations correspond thus to two age windows, from the Bashkirian to the Autunian (19 poles) and from the Middle Triassic to the Lias (4 poles). For the first window, the poles were obtained in different basins, widespread between the far western Tindouf and far eastern Murzuq ones, i.e., along a distance of about 2000 km. That gives an important significance to each of the data, which represent independent areas of the Saharan Platform. These poles were integrated in the classical paleomagnetic pole selection of McElhinny et al. (2003), Derder et al. (2006) and Torsvik et al. (2012) to determine (Le Goff et al. 1992) an improved APWP for the Gondwana (Amenna 2015).

However, a detailed comparison of the African paleomagnetic poles obtained in the Saharan basins with the Gondwana APWP highlighted an incoherency in the used selection. This incoherency appeared as due to the selected poles for South America (Tomezzoli et al. 2013). In fact, poles positions obtained from areas close to the eastern border of the Andean Cordillera are different from those obtained from the cratonic eastern part of this continent. This discrepancy pointed out tectonic disturbances not previously suspected in this border (Henry et al. 2017). The pole selection for the Gondwana, and therefore the Gondwana APWP, were then reevaluated and improved (Fig. 9).

Mainly due to the reliable paleomagnetic data from the Saharan basins, this APWP is very precise for the Upper Carboniferous, yielding a well-defined location of the Gondwana at this period (Fig. 10). By contrast, for the Laurussia, the limited number of available paleomagnetic data yields large uncertainty in its APWP (Domeier et al. 2012) and then of its location in the reconstruction. Because of the uncertainty in longitude in such reconstructions, other relative positions of the two supercontinents remain possible, and this reconstruction strongly argues for an A2 Pangea (Van der Voo and French 1974), as presented on the Fig. 10.

This APWP yielded also dating by comparison with the paleomagnetic data obtained in undated geological units (Fig. 11).

- K/Ar age of the dolerites studied in the Tin Serririne basin (Djellit et al. 2006) has been confirmed by this method (Derder et al. 2006).
- The Zarzaitine Formation, well dated in the Illizi basin (Lehman 1971; Bourquin et al. 2010; Aït Ouali et al. 2011), was studied in the Murzuq basin at Anaï area. Because of lack of paleontological arguments in this last basin, the age of this formation, at the base of the post-Hercynian deposits, was of particular interest.

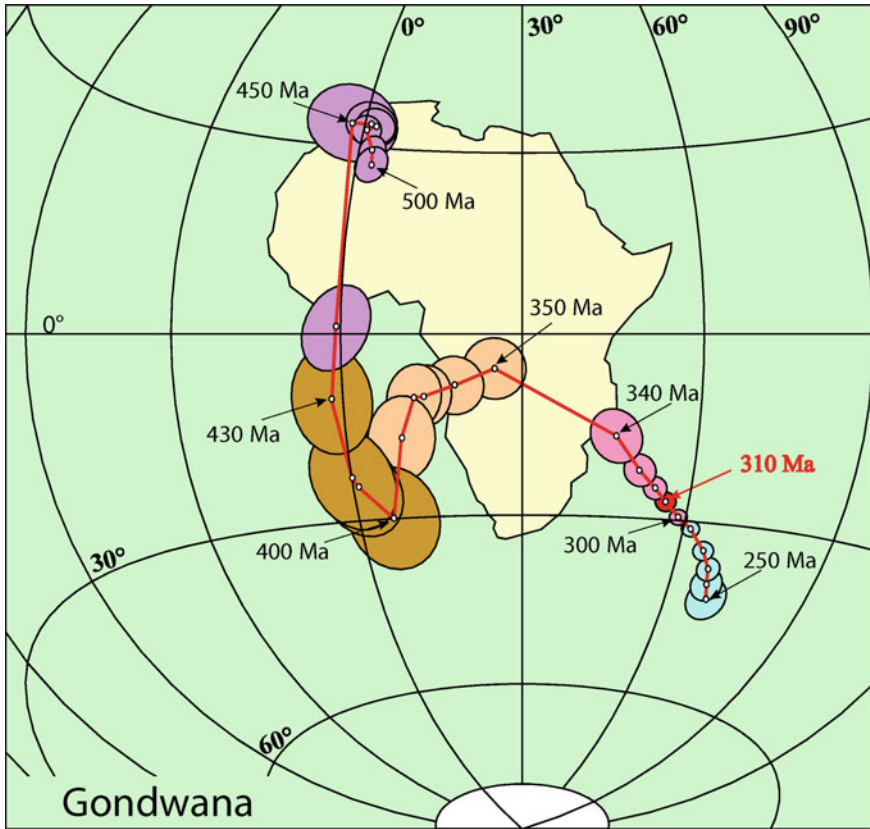


Fig. 9 Gondwana APWP (from Henry et al. 2017) for the period 500–250 Ma, with associated uncertainty zone at 95% A_{95} (Fisher 1953)

The obtained Late Permian age evidenced a very large diachronism (40 Ma) within the Zarzaitine Formation (Henry et al. 2014). This strong diachronism, as well as the local character of the Stephano–Autunian Tiguentourine deposits in newly formed basins in Libya (Hallett 2002), clearly indicates that the post-Hercynian structural evolution of the Saharan Platform included vertical movements, which gave differential uplifts. The latter was at the origin of erosion, hiatus or sediments deposition according to areas and likely according to time for a same area.

- The Lower Devonian age (415–400 Ma—Derder et al. 2016) of the very large sill discovered in the Murzuq basin shows that this magmatic event corresponds also to that (407 ± 8 Ma—Moreau et al. 1994) of the Aïr intrusives (Liégeois et al. 1994) and could be also at the origin of sand injections in different borders of the Murzuq basin (Moreau et al. 2012). In Niger, large sills in the same stratigraphical position (Menchikoff 1962) are probably of the same age. These

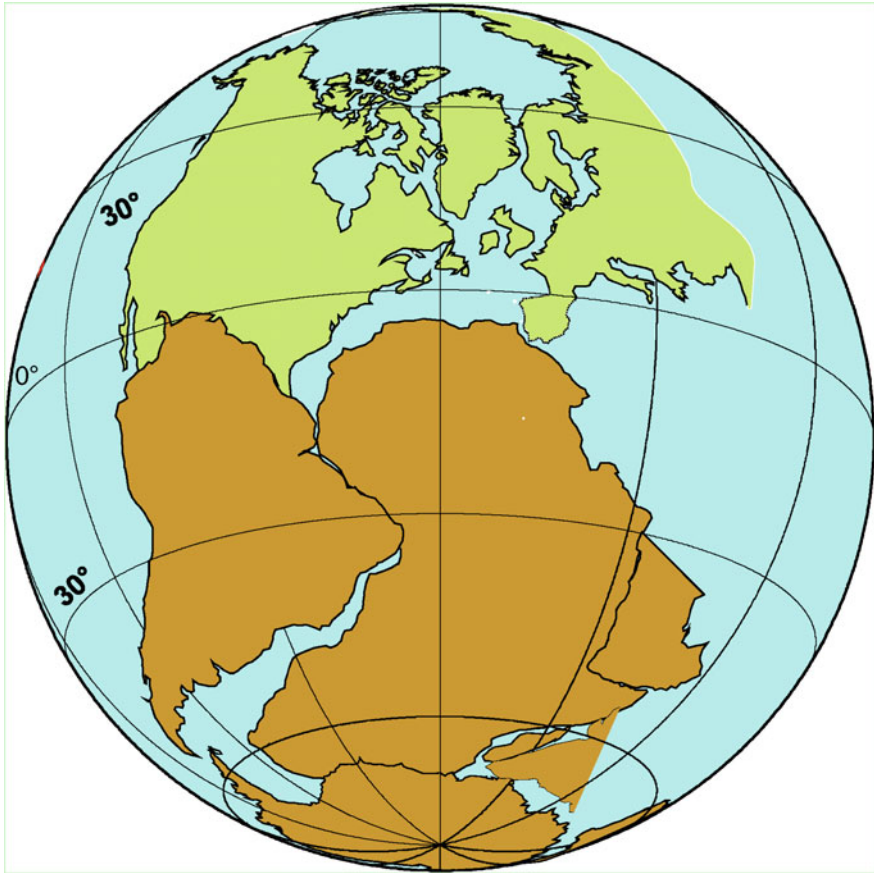


Fig. 10 Paleogeographic reconstruction for the Moscovian (310 Ma) using the data in north west African coordinates of Laurussia (Domeier et al. 2012) and Gondwana (Henry et al. 2017) to restore the landmasses independently. This reconstruction is in favor a Pangea A2 type, suggesting that such a reconstruction had existed since the Upper Carboniferous

different results imply a regional magmatic event affecting a very large area of the Saharan Platform. On the other hand, the loop of the Gondwana APWP (Fig. 9) between the Late Ordovician (pole 450 Ma) and Late Devonian (370 Ma) was not generally deemed as very reliable. The Aïr (Hargraves et al. 1987) and Arrikine (Derder et al. 2016) coherent mean paleomagnetic datum is “unique” and supports the existence of this loop, which has to be considered for the future paleocontinental reconstructions for this period.

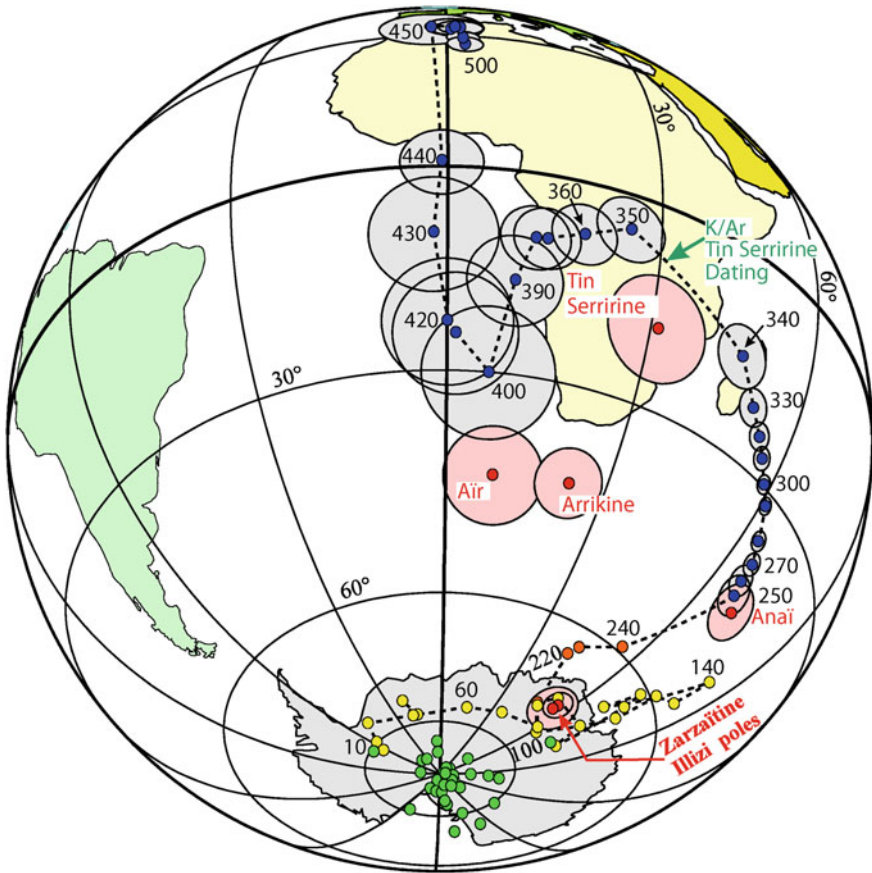


Fig. 11 Comparison of the Zarzaitine Illizi (Kies et al. 1995; Derder et al. 2001d), Anaï (Henry et al. 2014), Arrikine (Derder et al. 2016), Aïr (Hargraves et al. 1987) and Tin Serririne (Derder et al. 2006) paleomagnetic poles with the Gondwana and Africa APWP (500–250 Ma—Henry et al. 2017; 240–210 Ma—Domeier et al. 2012 and 200–0 Ma—Besse and Courtillot 2002). K/Ar age of the Tin Serririne dolerites (Djellit et al. 2006). “Cenozoic” remagnetizations poles from the Saharan basins are in green dots

6.2 Structural Implications

The study, in the Reggane basin, of a Jurassic sill emplaced within folded Paleozoic series, highlighted that actually part of this folding occurred after dolerites intrusion (Smith et al. 2006). The dip of the Paleozoic formations during intrusion has been determined by a small circles approach (see Henry et al. 2004a and references herein). It was interesting to notice that this dip had in some sites higher values than

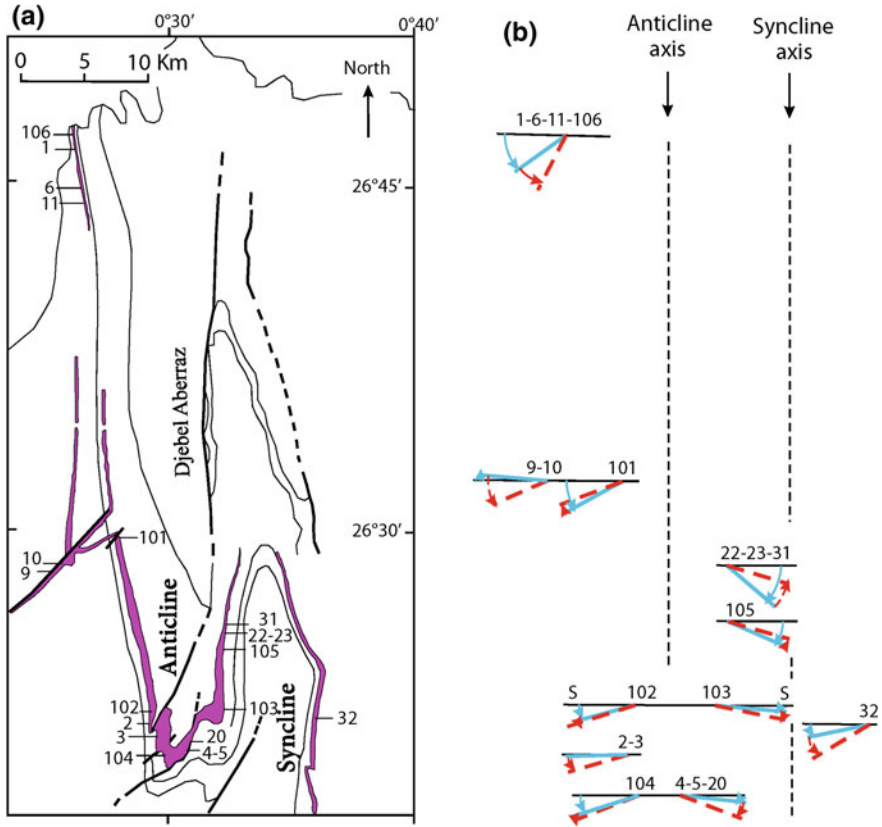


Fig. 12 **a** Sketch map of the Jurassic Reggane sill (pink color) area with the sites location and **b** dip values related to the two tilting events having occurred, respectively before (Hercynian dips, blue arrows) and after (red arrows) the dolerite emplacement for the different sites (from Fig. 11 of Smith et al. 2006)

the present dip (Fig. 12), implying locally tilting in opposite direction during the Hercynian and post-intrusion foldings. This proves the validity of the assumption of post-Hercynian tectonics in the Saharan Platform (Conrad 1972, 1981).

At Hassi Bachir area, Daly and Irving (1983) evidenced superimposition of paleomagnetic components. A new analysis (Derder et al. 2009) allowed isolation of the primary magnetization C and of another B component (possibly composite—see above). A statistical approach (Tauxe and Watson 1994), based on 10,000 bootstrap resamplings for progressive unfolding (Fig. 13), indicates that the B component is “syntectonic” (i.e., for paleomagnetists acquired either after the beginning of the first deformation and before the end of the last one, or during the folding in case of single tectonic event). This means that B component acquisition is related to the Hercynian folding or to existence of a second folding event, as shown with the Reggane dolerites.

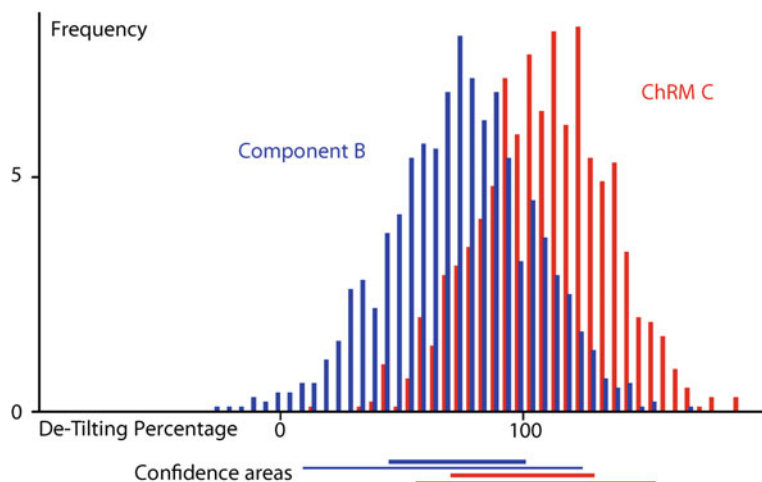


Fig. 13 Frequency (in percentage) of optimal untilting value (by window of 5°) obtained by the bootstrap method of Tauxe and Watson (1994) for B component (blue) and ChRM C (red), with confidence areas at 95% (thin line) and 63% (thick line), (from Fig. 7 of Derder et al. 2009)

Paleomagnetic data had also structural important implications in the “Ougarta” range, by pointing out two different tectonic phases affecting the magmatic complexes (Lamali et al. 2013).

6.3 Geochemical Implications

Remagnetizations phenomena, either partial or total, have been evidenced in many basins (e.g. Aifa 1993; Henry et al. 2004b). Only one Silurian site, metamorphized during the Arrikine sill intrusion (Murzuq basin), shows magnetic overprint related to heating (Derder et al. 2016). For the other studied geological units, the thickness of the overlying series at the time of remagnetization was insufficient to produce significant heating effects due to simple burial. In many areas, presence of high temperatures components of normal and reversed polarities during demagnetization process shows that remagnetizations are not related to effects of the recent field (Viscous Remanent Magnetization). Chemical phenomena represent, therefore, the main origin of the magnetic overprints of these different geological formations.

These overprints were acquired during two principal periods: the Permian and Cenozoic (Fig. 11). These two ages correspond in the Saharan Platform to erosion and continental environment. However, the presence of both magnetic polarities for the most recent remagnetizations in the different geological formations of the Illizi and Murzuq basins (Henry et al. 2004b; Lamali et al. 2014; Amenna et al. 2017) shows that they were not due to a simple superficial surface weathering. In addition, in the Illizi basin, a relation between the magnetic polarity and subhorizontal

stratigraphic levels (giving a pseudo-magnetostratigraphy) suggests a significant role of ground-fluids (Henry et al. 2004b). Both periods of remagnetization also correspond to differential uplifts in the Saharan Platform after the Hercynian main tectonics (Henry et al. 2014) or to the Cenozoic Hoggar uplift (Rougier et al. 2013). Fluids migration resulting from such vertical movements often favored chemical changes and remagnetization process (e.g., Oliver 1986; McCabe and Elmore 1989; Symons et al. 1996; Rouvier et al. 2001).

Paleomagnetic data yielded another geochemical implication. As mentioned above, the primary magnetization was not obtained in the studied sedimentary sites older than the Bashkirian of the Saharan basins. Indeed, all these rocks did not give stable remanent magnetization or were totally remagnetized. This Bashkirian age precisely corresponds to that obtained in the Arrikine sill by K/Ar (325.6 ± 7.7 Ma—Derder et al. 2016), age attributed to rejuvenation related to cryptocirculations of fluids, suggesting a significant regional geochemical event at this period.

7 Conclusion

More than a quarter century of paleomagnetic studies in Saharan basins surrounding the Hoggar Shield have largely contributed to a better knowledge of the Saharan Platform. These investigations demonstrated that the paleomagnetism is a strong tool for different geological and geodynamical purposes, being even in some cases the unique possible approach. Some applications, such as dating or tectonic analyses, used successfully in Algeria, could be applied in other countries of the Saharan Platform, thus opening other perspectives. As pointed out in this overview, analyses of rocks remagnetization and of their acquisition processes could have major geochemical implications. The remagnetizations, previously neglected by most paleomagnetists, could then become a new geochemical indicator. Finally, the example of the structural implications of the improvement of the South American APWP, mentioned in this overview, underlines that for tectonic purposes, it will be interesting to extend paleomagnetic investigations to the craton border zones, as around the south Atlasic flexure, which separates the Alpine domain from the Saharan craton in North Africa.

Acknowledgements We are very grateful to the Algerian research Ministry MESRS, to the French Foreign Office and to the French CNRS (Programs DPRS (DGRU)-CNRS, CMEP and PICS yielded financial supports). Special thanks also to the SONATRACH, ORGM, OPNA (Tamanrasset), ONPCT (Djanet) and to all the civil and military authorities everywhere in the Algerian Sahara for their constant and important help in the field. We are very grateful to Pr Mohamed Hamoudi for his detailed and constructive review.

References

- Aifa T (1993) Different styles of remagnetization in Devonian sediments from the north-western Sahara (Algeria). *Geophys J Int* 115:529–537
- Aifa T, Feinberg H, Pozzi JP (1990) Devonian/Carboniferous paleopoles for Africa. Consequences for Hercynian geodynamics. *Tectonophysics* 179:288–304
- Aït Ouali R, Nedjari A, Taquet P, Bitam L, Tayeb-Cherif L, Bouras R (2011) Le Zazaïtine inférieur (In Amenas, Sahara algérien): Derniers développements dans une série du Trias pro-parte. *Mém Serv Géol Natl* 17:6–26
- Amenna M (2009) Paléomagnétisme de formations sédimentaires paléozoïques du bassin de Tin Seririne et du bassin de l’Ahnet (Sud-Est et Nord-Ouest du Hoggar). Master thesis, USTHB University, Algiers
- Amenna M (2015) Applications du paléomagnétisme dans la bordure occidentale du bassin de Murzuq en Algérie. PhD thesis, U. S. T. H. B. University, Algiers
- Amenna M, Derder MEM, Henry B, Bayou B, Maouche S, Bouabdallah H, Ouabadi A, Beddiaf M, Ayache M (2014) Improved Moscovian part of the Gondwana APWP for paleocontinental reconstructions, obtained from a first paleomagnetic pole, age-constrained by a fold test, from In Ezzane area in the Murzuq basin (Algeria, Stable Africa). *J Afr Earth Sci* 99:342–352. <https://doi.org/10.1016/j.jafrearsci.2013.12.006>
- Amenna M, Derder MEM, Henry B, Maouche S, Bayou B, Ouabadi A, Bestandji R, Bouabdallah H, Ayache M, Beddiaf M (2017) Chemical remagnetization acquisition process: case study of the widespread Cenozoic remagnetization of the Saharan basins. *Arab J Geosci* 10:379. <https://doi.org/10.1007/s12517-017-3165-z>
- As JA, Zijderveld JDA (1958) Magnetic cleaning of rocks in paleomagnetic research. *Geophys J Roy Astron Soc* 1:308–319
- Bachtadse V, Briden JC (1991) Paleomagnetism of Devonian ring complexes from the Bayuda desert, Sudan—new constraints on the apparent polar wander path for Gondwanaland. *Geophys J Int* 104(3):635–646
- Bayou B, Smith B, Derder MEM, Yelles Chaouche K, Henry B, Djellit H (2000) Paleomagnetic investigations in Devonian rocks from the central Sahara, Algeria. In: Final proceeding of the first international symposium on geophysics, Tanta University, Egypt, 8–9 Sept 1998, pp 119–128
- Bayou B, Derder MEM, Henry B, Amenna M, Djellit H, Ouabadi A, Khaldi A, Baaziz K, Hemmi A (2004) Paléomagnétisme des Roches sédimentaires du Dévonien et volcaniques du Cambrien du bassin de Tin Seririne. In: Final proceeding of the international colloque: « Structure et Évolution de la Bordure Sud du Hoggar Central » C.R.A.A.G. and I.P.G.P., Algiers, 27 Nov 2004
- Bertrand JML, Caby R (1978) Geodynamic evolution of the Pan-African orogenic belt: a new interpretation of the Hoggar shield (Algerian Sahara). *Geol Rundsch* 67:357–388
- Besse J, Courtillot V (2002) Apparent and true polar wander and the geometry of the geomagnetic field over the last 200 Myr. *J Geophys Res* 107:2300. <https://doi.org/10.1029/2000JB000050>
- Beuf S, Biju-Duval B, de Charpal O, Rognon P, Gariel O, Benacef A (1971) Les grès du paléozoïque inférieur au Sahara; Sédimentation et discontinuités, évolution structurale d’un craton. Editions technip, Paris, pp 464–644
- Black R, Latouche L, Liégeois JP, Caby R, Bertrand JM (1994) Pan-African displaced terranes in the Tuareg shield (central Sahara). *Geology* 22:641–644
- Bouabdallah H, Henry B, Merabet NE, Maouche S (2003) Juxtaposed and superimposed magnetizations in Carboniferous formations of the Tindouf basin. *Bull Serv Cart Géol Algér* 14:53–64
- Boudzoumou F, Vandamme D, Affaton P, Gattacceca J (2011) Neoproterozoic paleomagnetic poles in the Taoudeni basin (west Africa). *C R Geosci* 343:284–294

- Bourquin S, Eschard R, Hamouche B (2010) High-resolution sequence stratigraphy of upper Triassic succession (Carnian–Rhaetian) of the Zarzaitine outcrops (Algeria): a model of fluvio-lacustrine deposits. *J Afr Earth Sci* 58:365–386
- Boussada MA, Merabet N, Mahdjoub Y, Maouche S, Chabou MC, Aifa T, Ayache M (2015) Paleomagnetic and magnetostructural study of the Gara Djebilet Jurassic magmatic formations (Tindouf Basin, Southwest Algeria). In: EGU General Assembly 2015, Vienne, Austria. Geophysical research abstracts, 17, pp EGU2015–2953, 2015
- Chabou MC (2008) Datation $^{39}\text{Ar}/^{40}\text{Ar}$ et Géochimie de la Province Magmatique de l'Atlantique Central dans le Sud-Ouest algérien. PhD thesis, Ecole Nationale Supérieure Polytechnique, Algiers
- Chabou MC, Sebai A, Féraud G, Bertrand H (2007) Datation $^{40}\text{Ar}/^{39}\text{Ar}$ de la province magmatique de l'Atlantique central dans le Sud-Ouest algérien. *C R Geosci* 339:970–978
- Conrad J (1972) Distension jurassique et tectonique éocrétacée sur le Nord-Ouest de la plate-forme africaine (Bassin de Reggane, Sahara central). *C R Acad Sci Paris* 274:2423–2426
- Conrad J (1981) La part des déformations posthercyniennes et de la néotectonique dans la structuration du Sahara central algérien, un domaine relativement mobile de la plate-forme africaine. *C R Acad Sci Paris* 292:1053–1056
- Conrad G, Le Mosquet Y (1984) Du craton vers sa marge : évolution sédimentaire et structurale du bassin Ahnet-Timimoun-Béchar (Sahara algérien) au cours du Carbonifère; données paléoclimatiques. *Bull Soc Géol Fr XXVI(6)*:987–994
- Daly L, Irving E (1983) Paléomagnétisme des roches carbonifères du Sahara central: analyse des aimantations juxtaposées: Configurations de la Pangée. *Ann Geophys* 1:207–216
- Derder MEM, Henry B, Mérabet N, Daly L (1994) Paleomagnetism of the Stephano-Autunian lower Tiguentourine formation from stable saharan craton (Algeria). *Geophys J Int* 116:12–22
- Derder MEM, Smith B, Henry B, Bayou B, Yelles Chaouche A, Djellit H, Ait Ouali A, Gandriche H (2001a) Juxtaposed and superimposed paleomagnetic components from the folded middle Carboniferous sediments in the Reggane basin (Saharan craton, Algeria). *Tectonophysics* 332:403–422
- Derder MEM, Henry B, Merabet N, Amenna M, Bourouis S (2001b) Upper Carboniferous paleomagnetic pole from stable Saharan craton and the Gondwana reconstructions. *J Afr Earth Sci* 32:491–502
- Derder MEM, Henry B, Bayou B, Amenna M, Djellit H (2001c) New Moscovian paleomagnetic pole from the Edjeleh fold (Saharan craton, Algeria). *Geophys J Int* 147:345–355
- Derder MEM, Henry B, Merabet N, Bayou B, Amenna M (2001d) Paleomagnetism of the Liassic member of the Zarzaitine formation (stable Saharan craton, Illizi basin, Algeria). *Ann Geofis* 44:995–1010
- Derder MEM, Henry B, Bayou B, Ouabadi A, Bellon H, Djellit H, Khaldi A, Amenna M, Baziz K, Hemmi A, Guemache MA (2006) New African lower Carboniferous paleomagnetic pole from intrusive rocks of the Tin Serririne basin (southern border of the Hoggar, Algeria). *Tectonophysics* 418:189–203
- Derder MEM, Henry B, Amenna M, Bayou B, Djellit H, Guemache MA, Hemmi A (2009) New structural implications for central Sahara (Algeria) from revisited upper Carboniferous “Hassi Bachir” formation: paleomagnetic constraints. *Tectonophysics* 463:69–76. <https://doi.org/10.1016/j.tecto.2008.09.012>
- Derder MEM, Maouche S, Liégeois JP, Henry B, Amenna M, Ouabadi A, Bellon H, Bruguier O, Bayou B, Bestandji R, Nouar O, Bouabdallah H, Ayache M, Beddiaf M (2016) Discovery of a Devonian mafic magmatism on the western border of the Murzuq basin (Saharan metacraton): paleomagnetic dating and geodynamical implications. *J Afr Earth Sci* 115:159–176
- Djellit H, Bellon H, Ouabadi A, Derder MEM, Henry B, Bayou B, Khaldi A, Baziz K, Merahi MK (2006) Age $^{40}\text{K}/^{40}\text{Ar}$, Carbonifère inférieur, du volcanisme basique filonien du synclinal paléozoïque de Tin Serririne, Sud-Est Hoggar (Algérie). *C R Geosci* 338:624–631
- Domeier M, Van der Voo R, Torsvik TH (2012) Paleomagnetism and Pangea: the road to reconciliation. *Tectonophysics* 514–517:14–43
- Fabre J (2005) Géologie du Sahara occidental et central. *Tervuren Afr Geosci Collect* 108:572p

- Fisher RA (1953) Dispersion on a sphere. *Proc Roy Soc Lond A* 217:295–305
- Freulon JM (1964) Etude géologique des séries primaires du Sahara central, Publ. du centre de Recherche Sahariennes (CNRS). *Serv Géol Algér* 3:1–198
- Galeazzi S, Point O, Haddadi N, Mather J, Druésne D (2010) Regional geology and petroleum systems of the Illizi-Berkine area of the Algerian Saharan Platform: an overview. *Mar Petrol Geol* 27:143–178
- Haddoum H, Guiraud R, Moussine-Pouchkine A (2001) Hercynian compressional deformations of the Ahnet-Mouydir basin, Algerian Saharan platform: far-field stress effects of the late palaeozoic orogeny. *Terra Nova* 13:220–226
- Hallett D (2002) *Petroleum geology of Libya*. Elsevier editors
- Halls HC (1976) A least squares method to find a remanence direction from converging remagnetization circles. *Geophys J Roy Astron Soc* 45:297–304
- Halls HC (1978) The use of converging remagnetization circles in paleomagnetism. *Phys Earth Planet Inter* 16:1–11
- Hargraves RB, Dawson EM, Houten FB, (1987) Palaeomagnetism and age of mid-palaeozoic ring complexes in Niger, West Africa, and tectonic implications. *Geophys Roy Astron Soc* 90:705–729. Doi:<https://doi.org/10.1111/j.1365-246x.1987.tb00750.x>
- Henry B, Merabet N, Yelles Chaouche A, Derder MEM, Daly L (1992) Geodynamical implications of a Moscovian palaeomagnetic pole from the stable Sahara craton (Illizi basin, Algeria). *Tectonophysics* 201:83–96
- Henry B, Merabet NE, Bouabdallah H, Maouche S (1999) Nouveau pôle paléomagnétique stéphanien inférieur pour le craton saharien (Formation de Merkala, bassin de Tindouf, Algérie). *C R Acad Sci Paris* 329(IIa):161–166
- Henry B, Rouvier H, Le Goff M (2004a) Using syntectonic remagnetizations for fold geometry and vertical axis rotation: example of the Cévennes border (France). *Geophys J Int* 157:1061–1070
- Henry B, Merabet N, Derder MEM, Bayou B (2004b) Chemical remagnetizations in the Illizi basin (Saharan craton, Algeria). *Geophys J Int* 156:200–212
- Henry B, Derder MEM, Amenna M, Maouche S, Bayou B, Ouabadi A, Bouabdallah H, Ayache M, Beddiaf M, Bestandji R (2014) Paleomagnetic dating of continental geological formations: strong diachronism evidenced in the Saharan platform and geodynamical implications. *J Afr Earth Sci* 99:353–362. <https://doi.org/10.1016/j.jafrearsci.2014.02.010>
- Henry B, Derder MEM, Amenna M, Maouche S, Bayou B (2017) Better constrained selection of the paleozoic west Gondwana (South America) paleomagnetic poles for the APWPs determination. *Stud Geophys Geod* 61. <https://doi.org/10.1007/s11200-016-1036-9>
- Kent DV, Dia O, Sougy JMA (1984) Paleomagnetism of lower-middle Devonian and upper Proterozoic-Cambrian(?) rocks from Mejeria (Mauritania, West Africa), In: Van der Voo R, Scotese CR, Bonhommet N (eds) *Plate reconstruction from Paleozoic paleomagnetism*. AGU Geodynamics series, vol 12, pp 99–115
- Kherroubi A (2003) *Paléomagnétisme des formations paléozoïques des bassins Ouest Sahariens*. Master thesis, USTHB Houari Boumediene University, Algiers
- Kies B, Henry B, Merabet N, Derder MEM, Daly L (1995) A new late Triassic-Liasic paleomagnetic pole from superimposed and juxtaposed magnetizations in the Saharan craton. *Geophys J Int* 120:433–444
- Kirschvink JL (1980) The least-squares line and plane analysis of palaeomagnetic data. *Geophys J Roy Astron Soc* 62:699–718
- Lamali A, Merabet N, Henry B, Maouche S, Graine-Tazerout K, Mekkaoui A, Ayache M (2013) Polyphased geodynamical evolution of the Ougarta (Algeria) magmatic complexes evidenced by paleomagnetic and AMS studies. *Tectonophysics* 588:82–89
- Lamali A, Merabet N, Henry B, Maouche S, Hamoudi M, Ayache M (2014) Réaimantations énigmatiques des formations du Silurien et du Dévonien inférieur du Tassili N-Ajjer (Bassin d'Illizi, Algérie). *Bull Serv Géol Natl Algér* 25:181–199
- Le Goff M, Henry B, Daly L (1992) Practical method for drawing VGP paths. *Phys Earth Planet Inter* 70:201–204

- Lehman JP (1971) Nouveaux vertébrés du Trias de la série du « Zarzaïtine ». *Ann Paléont Vertébr Paris* 57:71–93
- Liégeois JP, Black R, Navez J, Latouche L (1994) Early and late Pan-African orogenies in the Air assembly of terranes (Tuareg shield, Niger). *Precambr Res* 67:59–66
- Liégeois J-P, Benhallou A, Azzouni-Sekkal A, Yahiaoui R, Bonin B (2005) The Hoggar swell and volcanism: reactivation of the precambrian Tuareg shield during Alpine convergence and West African Cenozoic volcanism. In: Foulger GR, Natland JH, Presnall DC, Anderson DL (eds) *Plates, plumes, and paradigms*, vol 388. Geological Society of America special paper, pp 379–400
- McCabe C, Elmore RD (1989) The occurrence and origin of late Paleozoic remagnetization in the sedimentary rocks of North America. *Rev Geophys* 27:471–494
- McElhinny MW (1964) Statistical significance of the fold test in palaeomagnetism. *Geophys J Roy Astron Soc* 8:338–340
- McElhinny MW, Powell C McA, Pisarevsky SA (2003) Paleozoic terranes of eastern Australia and the drift history of Gondwana. *Tectonophysics* 362:41–65
- McFadden PL (1990) A new fold test for palaeomagnetic studies. *Geophys J Int* 103:163–169
- McFadden PL, McElhinny MW (1988) The combined analysis of remagnetization circles and direct observations in palaeomagnetism. *Earth Planet Sci Lett* 87:161–172
- McFadden PL, McElhinny MW (1990) Classification of the reversal test in palaeomagnetism. *Geophys J Int* 103:725–729
- Menchikoff N (1962) Carte géologique du Nord-Ouest de l’Afrique: Sahara central. CNRS
- Merabet N, Bouabdallah H, Henry B (1998) Paleomagnetism of the lower Permian redbeds of the Abadla basin (Algeria). *Tectonophysics* 293:127–136
- Merabet N, Henry B, Bouabdallah H, Maouche S (1999) Paleomagnetism of the Djebel Reouina Namurian formation (Tindouf basin, Algeria). *Stud Geophys Geod* 43:376–389
- Merabet N, Kherroubi A, Maouche S, Henry B (2000) Paleomagnetism of the Permian series of the Mezarif basin (Algeria). *Geol Carpath* 51:179
- Merabet N, Henry B, Kherroubi A, Maouche S (2005) Autunian age constrained by fold tests for paleomagnetic pole from Mezarif and Abadla basins (Algeria). *J Afr Earth Sci* 43:556–566
- Moreau C, Demaiffe D, Bellion Y, Boullier AM (1994) A tectonic model for the location of Paleozoic ring-complexes in Air (Niger, West Africa). *Tectonophysics* 234:129–146
- Moreau J, Ghienne JF, Hurst A (2012) Kilometre-scale sand injectites in the intracratonic Murzuq basin (south-west Libya): an igneous trigger? *Sedimentology* 59:1321–1344
- Morel P, Irving E (1981) Paleomagnetism and the evolution of Pangea. *J Geophys Res* 86 (B3):1858–1872
- Morel P, Irving E, Daly L, Moussine-Pouchkine A (1981) Paleomagnetic results from Permian rocks of the northern Saharan craton and motions of the Moroccan Meseta and Pangea. *Earth Planet Sci Lett* 55:65–74
- Nedjari A, Aït Ouali R, Debaghi F, Hamdidouche R, Benhamouche A, Amrouche F, Messamri K (2011) La Géologie Saharienne Revisitée (1980–2009). *Mém Serv Géol Natl* 17:85–176
- Oliver J (1986) Fluids expelled tectonically from orogenic belts: their role in hydrocarbon migration and other geologic phenomena. *Geology* 14:99–102
- Rougier S, Missenard Y, Gautheron C, Barbarand J, Zeyen H, Pinna R, Liégeois JP, Bonin B, Ouabadi A, Derder MEM, Frizon de Lamotte D (2013) Eocene exhumation of the Tuareg Shield (Sahara Desert, Africa). *Geology* 41:615–618. <https://doi.org/10.1130/G33731.1>
- Rouvier H, Henry B, Macquar JC, Leach D, Le Goff M, Thibérioz J, Lewchuk MT (2001) Réaimantation régionale éocène, migration de fluides et minéralisations dans la bordure cévenole. *Bull Soc Géol Fr* 172:503–516
- Schmidt PW, Clark DA (2000) Paleomagnetism apparent polar wander path and paleolatitude. In: Veevers JJ (ed) *Billion year earth history of Australia and neighbours in Gondwanaland*. GEOMOG Press, Department of Earth and Planetary Sciences, Macquarie University, Sydney, pp 12–17
- Shipunov SV (1997) Synfolding magnetization: detection testing and geological applications. *Geophys J Int* 130:405–410

- Smith AG, Hallam A (1970) The fit of the southern continents. *Nature* 225(5228):139–144
- Smith AG, Hurley AM, Briden JC (1981) Phanerozoic paleocontinental world maps. Cambridge Univ. Press, London, UK
- Smith B, Moussine-Pouchkine A, Ait Kaci A (1994) Paleomagnetic investigation of middle Devonian limestones of Algeria and the Gondwana reconstruction. *Geophys J Int* 119:166–186
- Smith B, Derder MEM, Henry B, Bayou B, Amenna M, Djellit H, Yelles AK, Garces M, Beamud E, Callot JP, Eschard R, Chambers A, Aifa T, Ait Ouali R, Gandriche H (2006) Relative importance of the Hercynian and post-Jurassic tectonic phases in the Saharan platform: a palaeomagnetic study of Jurassic sills in the Reggane basin (Algeria). *Geophys J Int* 167:380–396
- Symons DTA, Sangster DF, Leach D (1996) Paleomagnetic dating of Mississippi valley-type Pb-Zn-Ba deposits. In: Sangster DF (ed) Carbonate hosted Pb/Zn deposits, special vol 4. Society of Economic Geologists
- Tauxe L, Watson GS (1994) The fold test: an eigen analysis approach. *Earth Planet Sci Lett* 122:331–341
- Tomezzoli RN, Vizán H, Tickyj H, Woroszylo ME (2013) Revisión de la posición del polo paleomagnético de Sierra Chica en la curva de desplazamiento polar aparente del Gondwana. *Latinmag Lett* 3(Special Issue, OB25):1–8. <http://www.geofisica.unam.mx/LatinmagLetters/LL13-03-SP/LLv3spIndex.html>
- Torcq F, Besse J, Vaslet D, Marcoux J, Ricou LE, Halawani M, Basahel M (1997) Paleomagnetic results from Saudi Arabia and the Permo-Triassic Pangea configuration. *Earth Planet Sci Lett* 148:553–567, 1997
- Torsvik TH, Van der Voo R, Preeden U, Mac Niocaill C, Steinberger B, Doubrovine PV, van Hinsbergen DJJ, Domeier M, Gaina C, Tohver E, Meert JG, McCausland PJA, Cocks LRM (2012) Phanerozoic polar wander, paleogeography and dynamics. *Earth Sci Rev* 114:325–368. <https://doi.org/10.1016/j.earscirev.2012.06.007>
- Van der Voo R (1990) The reliability of paleomagnetic data. *Tectonophysics* 184:1–9
- Van der Voo R (1993) Paleomagnetism of the Atlantic, Tethys and Iapetus oceans. Cambridge University Press, 441 pp
- Van der Voo R, French RB (1974) Apparent polar wandering for the Atlantic-bordering continents: late Carboniferous to Eocene. *Earth Sci Rev* 10:99–119
- Waldhör M, Appel E (2006) Intersections of remanence small circles: new tools to improve data processing and interpretation in palaeomagnetism. *Geophys J Int* 166:33–45
- Zijderveld JDA (1967) Demagnetization of rocks: analysis of results. In: Collision DW, Creer KM, Runcorn SK (eds) *Methods in paleomagnetism*, pp 254–286